

# Ge condensation under SiGe oxidization: from Molecular Dynamics simulation to one-dimensional analytic modeling.

Patrick Ganster,<sup>1</sup> Andrès Saúl,<sup>1, a)</sup> and Guy Trégliá,<sup>1, b)</sup>

CINaM, UMR 7325 CNRS, Aix-Marseille University, Campus de Luminy, 13288 Marseille cedex 9, France<sup>c)</sup>

(Dated: 20 September 2018)

Oxidization of a dilute Si(Ge) alloy is modeled using an original protocol based on molecular dynamics simulation and rules for the oxygen insertions. These rules, deduced from *ab-initio* calculations, favor the formation of SiO<sub>2</sub> against GeO<sub>2</sub> oxide which leads to segregation of Ge atoms into the alloy during the oxidization front advance. Ge condensation is then observed close to the SiO<sub>2</sub>/Ge interface due to the strain induced by oxydization in this region. From the analysis of the simulation process, we propose a one-dimensional description of Ge condensation wich perfectly reproduces the evolution of the Ge concentration during oxidization of the SiGe alloy.

PACS numbers: Valid PACS appear here

Keywords: Suggested keywords

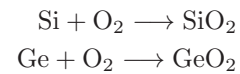
In the challenging world of nanotechnologies, the so-called, Ge-condensation technique, is a promising way to realize thin Ge layers of good quality for high mobility MOSFET channel<sup>1</sup>. The method consists in oxidizing at high temperature an Si<sub>1-x</sub>Ge<sub>x</sub> alloy epitaxially grown on SOI substrate and preliminary capped by a thin silicon layer. After the oxidization of the silicon cap that forms SiO<sub>2</sub> oxide, the pursuit of oxidization induces the segregation of Ge atoms in the SiGe alloy which becomes enriched in Ge.

The development of predicting numerical tools to optimize manufacturing steps<sup>2</sup> is essential and necessary to get a good understanding of the relevant mechanisms involved during the Ge-condensation process. In the context of the continuous decrease of the microsystem sizes and the use of smaller quantities of matter, descriptions and precise characterizations at the atomic scale is a necessary road map to progress in the understanding of the driving mechanisms involved in the Ge condensation technique. Such an atomistic description is a challenging problem which needs to deal with a complex system and many mechanisms occurring at the same time. In particular, it requires to model the oxidization of the SiGe alloy and the segregation of Ge atoms from the oxydised region to the substrate. A full description taking into account all mechanisms and reproducing the time evolution of the system in one model is obviously far from the actual state-of-art of computational science at atomic scales.

In this letter, we propose an atomistic model which couples molecular dynamics simulations and rules deduced from *ab-initio* calculations to model oxidization of SiGe alloy involving the Ge segregation. In order to

be able to describe a system sufficiently large to be representative of the Ge condensation, we use the Stillinger-Weber (SW) empirical potential which has been successfully employed and optimized to describe SiGe alloys and Si-O mixed systems by Molecular Dynamics or Monte Carlo simulation<sup>3-9</sup>. The parameters of this potential, which is composed of 2-body and 3-body interactions, were fitted to *ab-initio* calculations and thermodynamical properties of Si, Ge, and SiGe compounds. For the mixed Si-Ge-O system, we derived a set of parameters from those developed by Watanabe *et al.*<sup>7</sup> and Clancy *et al.*<sup>6</sup> to study respectively Si-O and a SiGe. In practice, for the Ge-O interactions, we scaled the SW parametrization of Watanabe *et al.* by using the size and energy parameters of the Ge parametrization developed by Clancy *et al.*<sup>6</sup>. Arithmetical and geometrical averages have been used for the size and energy parameters respectively the in 3-body interactions involving triplets composed of Si, O and Ge atoms such as OSiGe, SiSiGe, SiOGe, ...

As mentioned above, the Ge condensation process begins by the oxidization of the silicon cap covering the SiGe alloy. This step is essential since it initiates the formation of a SiO<sub>2</sub> oxide<sup>10</sup>. After the oxidation of the whole silicon cap, one would expect the formation of either SiO<sub>2</sub>, GeO<sub>2</sub> or a mixed SiO<sub>2</sub>-GeO<sub>2</sub> amorphous oxide. However, the experiments show a preferential oxidization of the Si atoms which induces the segregation of Ge atoms and an increase of the fraction of Ge in the SiGe alloy<sup>1,11</sup>. This preferential oxydization, can be understood from the differential in formation energy  $E_f$  between SiO<sub>2</sub> and GeO<sub>2</sub> in the  $\alpha$ -quartz phases :



From the total energies obtained using the WIEN2K code<sup>12</sup> the formation energy can be calculated as :

$$E_f^{\text{XO}_2} = E^{\text{XO}_2} - E^{\text{X}} - E^{\text{O}_2} \quad (1)$$

<sup>a)</sup>email: saul@cinam.univ-mrs.fr

<sup>b)</sup>email: treglia@cinam.univ-mrs.fr

<sup>c)</sup>email: ganster@emse.fr; Present address: MSE, SMS-MPI, 158 cours Fauriel, 42023 Saint-Etienne Cedex 2, France

where  $E^{XO_2}$  is the total energy of the oxide,  $E^X$  is the energy of  $X = \text{Si}$  or  $\text{Ge}$  in the diamond phase structure and  $E^{O_2}$  the energy of an isolated  $O_2$  molecule. We have found that the  $E_f^{SiO_2}$  is much lower than  $E_f^{GeO_2}$ , respectively -8.2 eV and -4.7 eV<sup>13</sup>, in full qualitative agreement with experimental observation since  $\Delta = E_f^{GeO_2} - E_f^{SiO_2} = 3.5$  eV implies that the formation of  $SiO_2$  is highly favored against that of  $GeO_2$ .

The validity of our parametrization of the semi-empirical SW potential was also checked on its ability to describe this preferential oxydation. The difference between the formation energy of  $SiO_2$  and  $GeO_2$  was found to be  $\Delta = 1.8$  eV, which is half the value obtained by the *ab-initio* calculations, but widely sufficient to ensure the empirical model to clearly favor the formation of  $SiO_2$  against  $GeO_2$  phase.

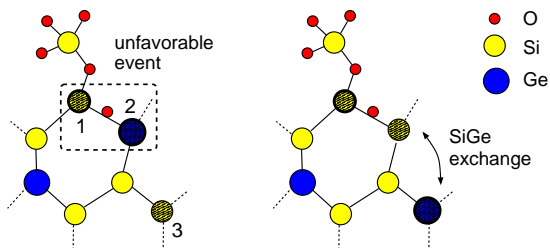


FIG. 1. (color online) Scheme of the oxygen insertion taking into account the preferably oxydization of the Si atom i) the highest Si in the substrate surrounded by at least one and at most three oxygen atoms is located (yellow circle labeled 1), ii) when the last chance to introduce oxygen is on a Si-Ge bond, the considered Ge atom (bleu circle numbered 2) is exchanged with a non-oxidized Si atom of the substrate (yellow circle labeled 3).

The simulation box that we have used was oriented in such a way that the  $x$ -,  $y$ -, and  $z$ -axis of the simulation box are along the  $\langle 100 \rangle$  directions of the diamond lattice. The system size is  $27.15 \times 27.15 \times 108.6 \text{ \AA}^3$ . Periodic boundary conditions were applied in the  $[100]$  and  $[010]$  directions (*i.e.*  $x$  and  $y$ ) and the system was free to relax in the  $[001]$  direction (free surfaces). The starting configuration was a bare  $Si_{0.95}Ge_{0.05}$  substrate (3700 Si and 194 Ge atoms), which was capped by a pure Si layer in the upper part (300 Si additional atoms).

To simulate SiGe oxydization, we use a protocol based on molecular dynamics (MD) simulations and on the one-by-one incorporation of oxygen atoms into Si-Si bonds. This protocole is an extension to the one that we have previously used in the case of Si oxydization<sup>9</sup>. We take now into account the preferential formation of  $SiO_2$  against  $GeO_2$  oxide. In order to simulate the initial nuclei of the oxydization process, oxygen atoms are placed on 10 % of the Si dangling bonds (randomly chosen) on top of the cap Si layer, which is not reconstructed before the oxygen insertion. This initial configuration is equilibrated at 1200 K during 20 ps by rescaling the atomic velocities every 0.5 ps. Then, we include the oxygen atoms one by one following the following sequence. We search

for the highest Si atom in the substrate which is bound to at least one and at most three oxygen atoms and the oxygen atom is placed in the middle of the longest Si-Si bond available around this Si atom<sup>9</sup>. When only a Si-Ge bond is found, we place the oxygen atom in the middle of the bond and we exchange the Ge atom with a non-oxidized Si atom of the SiGe substrate. The latter being determined in order to be the most energetically favorable exchange. This procedure is schematized in the Fig. 1. The whole system is relaxed by a Molecular Dynamic run at 1200 K during 1 ps. The full scheme (insertion, relaxation) is repeated for 6000 oxygen atoms insertions during which some 600-700 Si-Ge exchanges were realized. This procedure leads to the formation of a pure amorphous  $SiO_2$  oxide which is composed of a random network of  $SiO_4$  entities connected by vertex, which is very similar to that of the  $SiO_2/Si$  system<sup>9</sup>.

The Ge concentration profile along the  $z$ -axis below the  $SiO_2/SiGe$  interface for a typical run is shown in Fig. 2 after different oxydation steps (5, 2000, 4000, and 6000 oxygen insertions). The concentration is defined for diffuse layers of thickness  $\Delta z = 1 \text{ \AA}$ . Starting from an uni-

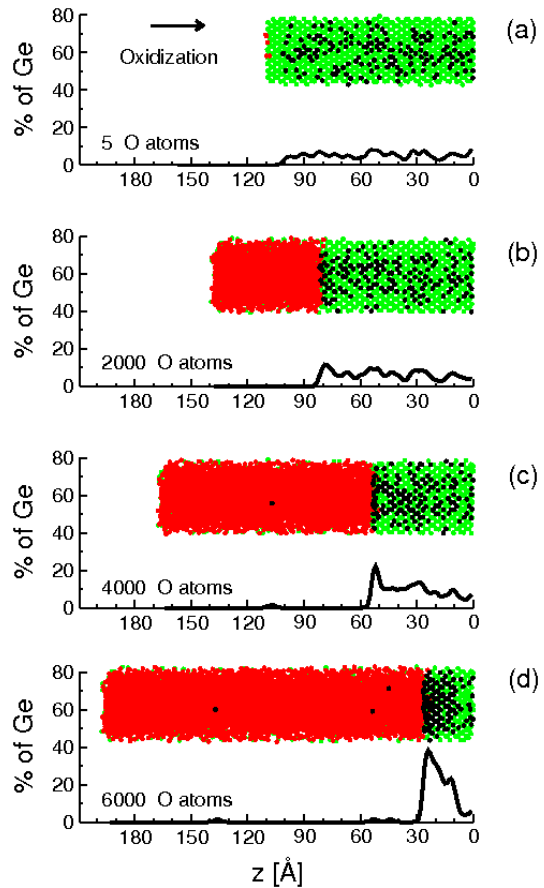


FIG. 2. (color online) Evolution of the Ge concentration  $n_{Ge}/(n_{Ge} + n_{Si})$  profile for the  $SiO_2/SiGe$  system after insertion of 5, 2000, 4000, and 6000 oxygen atoms. O, Si and Ge atoms are represented in red, green and black respectively.

form concentration of Ge along the  $z$ -axis (Fig. 2(a)), one can see that the Ge atoms concentrate in the vicinity of the interface between  $\text{SiO}_2$  and SiGe (Fig. 2(b)-(d)), in good agreement with RBS measurements<sup>14</sup>.

The overall picture is that the oxidation evolves by pushing a Ge strip which thickens all along the process, whilst preserving a concentration lower than 50 % per plane. This means that the Ge atoms expelled from the oxide mainly exchange with Si substrate atoms located close to the  $\text{SiO}_2/\text{SiGe}$  interface, even though a few exchanges also involve Si atoms far from this interface, leading to a slight increase of the overall Ge concentration.

This qualitative behaviour can be confirmed by analyzing the relative position of the Si and Ge atoms which are exchanged during the oxidation process. In Fig. 3 we show an histogram of the projections of the distance parallel  $d_{\parallel}$  and perpendicular  $d_{\perp}$  to the interface. The distribution of  $d_{\parallel}$  is uniform and does not exceed half the size of the simulation box, which indicates that exchanges occur between Si and Ge atoms ranging for all the simulation box width. On the contrary, the distribution of  $d_{\perp}$  presents a narrow peak which is almost completely damped beyond 5 Å which corresponds to three (001) interatomic layers. This shows that the Ge atoms mainly exchange with Si atoms located in the vicinity of the  $\text{SiO}_2/\text{SiGe}$  interface, which leads to their accumulation (condensation) in this limited region. The tail of the distribution of  $d_{\perp}$  towards larger distances confirms that a few exchanges can also occur between more distant Si and Ge atoms, leading to the slight increase in the overall Ge concentration profile.

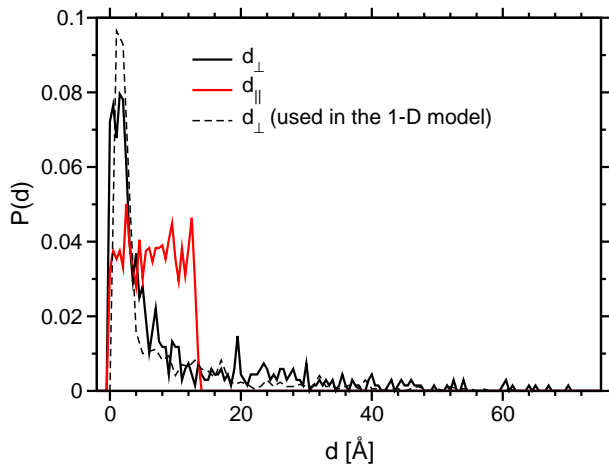


FIG. 3. (color online) Distribution of the parallel  $d_{\parallel}$  and perpendicular  $d_{\perp}$  projections of the distances separating exchanged Si and Ge atoms during the oxidation process.

It remains to identify the physical origin of the preference for Si-Ge exchanges to occur close to the interface. A careful analysis of the local concentrations does not allow to establish any correlation between the Ge concentration in the SiGe substrate and the new local environment of the exchanged Ge atom. However, we have

found that this preference is induced by the strain originated by the oxidation in the interfacial region. In Fig. 4 we show the pressure maps averaged over the first three SiGe layers below the oxidation front after insertion of 2000, 4000 and 6000 oxygen atoms. These two dimensional maps, parallel to the interface, are very similar at each step of the process and reveal an inhomogeneous strain distribution which is rapidly damped beyond these three layers. More precisely, one sees that tensile and compressive regions coexist in almost equal proportions. The Ge condensation close to the interface is then originated by the segregation of the "big" Ge atoms (the size-mismatch between Si and Ge is of about 4 %) in the tensile regions. The number of tensile sites decreases when the Ge concentration increases and should disappear when the concentration reaches 50%. This is indeed what is observed in Fig. 2(d), confirming the strain origin of Ge condensation close to  $\text{SiO}_2/\text{SiGe}$  interface.

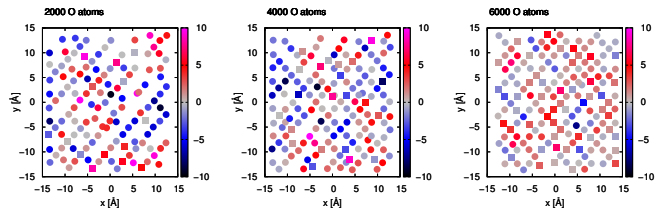


FIG. 4. (color online) Lateral stress maps of the first three layers below the  $\text{SiO}_2/\text{SiGe}$  interface after insertion of 2000, 4000 and 6000 oxygen atoms. Tensile and compressive regions are represented in blue and red respectively.

From the previous analysis, it is clear that one of the essential ingredients which are responsible of the Ge condensation, is the peculiar distribution of distances between exchanged Si-Ge atoms displayed in Fig. 3). A simple one dimensional model of Ge condensation can be used to understand the role played by the overall shape of this distribution. Let us consider a non-oxidized SiGe substrate composed of  $N$  layers labelled  $p$  ( $p = 1, N$ ), each layer contains a finite number of atoms  $n(p) = n_{\text{Ge}}(p) + n_{\text{Si}}(p)$  where  $n_{\text{Ge}}(p)$  and  $n_{\text{Si}}(p)$  are respectively the number of Ge and Si atoms in the  $p$  layer. Assuming that oxidation is progressing layer-by-layers, by exchanging Ge atoms from the first  $p$  layers, starting from  $p = 1$ , with Si atoms of deeper layers, distant by  $d_{\perp}$  from the former, the Ge condensation follows the simple set of equations :

$$n_{\text{Ge}}(p) = n_{\text{Ge}}(p) - 1 \quad (2)$$

$$n_{\text{Si}}(p) = n_{\text{Si}}(p) + 1 \quad (3)$$

$$n_{\text{Ge}}(p + d_{\perp}) = n_{\text{Ge}}(p + d_{\perp}) + 1 \quad (4)$$

$$n_{\text{Si}}(p + d_{\perp}) = n_{\text{Si}}(p + d_{\perp}) - 1 \quad (5)$$

Starting from the same initial Ge concentration 5 %, number of atoms per layer  $n(p) = 50$  and number of SiGe layers  $N = 72$  than in the MD simulation, the Equations

(2)-(5) lead to the evolution of the Ge concentration profiles displayed in Fig. 5. The inset in this figure recalls the probability distribution of the interlayer distance  $d_{\perp}$  between the exchanged Si and Ge atoms which is used in the simulation, i.e., for each exchange we randomly choose a  $d_{\perp}$  following this distribution.

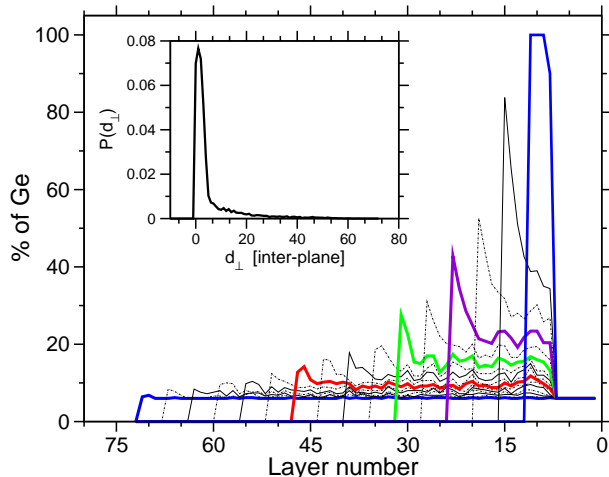


FIG. 5. Ge concentration after each four layers depleted in Ge. The inset shows the distribution of SiGe exchanged during the simulation.

As can be seen, this simple model reproduces the essential features of the MD model, namely the formation of a Ge strip below the  $\text{SiO}_2/\text{SiGe}$  interface, which thickens as oxidation goes along. However, the model misses the saturation of Ge segregation at about 50 % per plane.

To summarize, we have shown here by using atomistic models combining *ab-initio* and empirical potentials), that the main driving force for Ge condensation under oxidation are the preferential  $\text{SiO}_2$  formation against that of  $\text{GeO}_2$  and the existence of an inhomogeneous strain ex-

tending on a few layers below this interface. The latter effect is at the origin of the localisation of the Ge aggregates close to the interface. In addition, we have shown that a simple 1D model, based on the single knowledge of the distribution of distance between Ge and Si atoms exchanged during the simulation (related to the strain distribution), is sufficient to account for the main features of Ge condensation, providing us a flexible method to study this phenomenon under various conditions.

- <sup>1</sup>S. Dissanayake, Y. Shuto, S. Sugahara, M. Takenaka, and S. Takagi, *Thin Solid Films* **517**, 178 (2008).
- <sup>2</sup>W. Fichtner, *J. Comp. Th. Nanosci.* **5**, 1089 (2008).
- <sup>3</sup>S. Krishnan, L. Henet, T. Key, B. Glorieux, M.-L. Saboungi, and D. L. Price, *Journal of Non-Crystalline Solids* **353**, 2975 (2007).
- <sup>4</sup>C. Tzoumanekas and P. C. Kelires, *Journal of Non-Crystalline Solids* **266-269**, 670 (2000).
- <sup>5</sup>Q. Yu, M. O. Thompson, and P. Clancy, *Phys. Rev. B* **53**, 8386 (1996).
- <sup>6</sup>Q. Yu and P. Clancy, *Modelling Simul. Sci. Eng.* **2**, 829 (1994).
- <sup>7</sup>T. Watanabe, H. Fujiwara, H. Noguchi, T. Hoshino, and I. Ohdomari, *Jpn. J. Appl. Phys.* **38**, L366 (1999).
- <sup>8</sup>J. D. Torre, J.-L. Bocquet, Y. Limoge, J.-P. Crocombette, E. Adam, G. Martin, T. Baron, P. Rivallin, and P. Mur, *J. of Appl. Phys.* **92**, 1084 (2002).
- <sup>9</sup>P. Ganster, G. Tréglia, F. Lançon, and P. Pochet, *Thin Solids Films* **518**, 2422 (2010).
- <sup>10</sup>Z. Di, M. Zhang, W. Liu, M. Zhu, C. Lin, and P. K. Chu, *Materials Science and Engineering: B* **124-125**, 153 (2005).
- <sup>11</sup>Q. Li, A. Navrotsky, F. Rey, and A. Corma, *Microporous and Mesoporous Materials* **64**, 127 (2003).
- <sup>12</sup>The WIEN2K program is an implementation of the full-potential linearized augmented plane-wave method based on density-functional theory. P. Blaha, K. Schwarz, G. Madsen, D. Kvaniscka, and J. Luitz, in *Wien2k, An Augmented Plane Wave Plus Local Orbitals Program for Calculating Crystal Properties*, edited by K. Schwarz Vienna University of Technology, Vienna, Austria, 2001.
- <sup>13</sup>The calculations presented here were performed using the generalized gradient approximation of Perdew, Burke, and Ernzerhof<sup>2</sup> (GGA) for exchange and correlation and a cut-off parameter  $RK_{\max} = 8$ .
- <sup>14</sup>F. K. LeGoues, R. Rosenberg, and B. S. Meyerson, *Applied Physics Letters* **54**, 644 (1989).